Li, T.-K., & Magnes, L. J. (1975) *Biochem. Biophys. Res. Commun. 63*, 202–208.
Li, T.-K., Bosron, W. F., Dafeldecker, W. P., Lange, L. G., & Vallee, B. L. (1977) *Proc. Natl. Acad. Sci. U.S.A. 74*, 4378–4381.
Lowry, O. H., Rosebrough, N. J., Farr, A. L., & Randall, R. J. (1951) *J. Biol. Chem. 193*, 265–275.
Lutstorf, U. U., Schürch, P. M., & von Wartburg, J.-P. (1970) *Eur. J. Biochem. 17*, 497–508.
Pares, X., & Vallee, B. L. (1981) *Biochem. Biophys. Res. Commun. 98*, 121–130.
Pietruszko, R. (1975) in *Isozymes* (Markert, C. L., Ed.) Vol. 1, pp 707–724, Academic Press, New York.
Pietruszko, R. (1979) in *Biochemistry and Pharmacology of Ethanol* (Majchrowicz, E., & Noble, E. P., Eds.) Vol. 1, pp 87–106, Plenum Press, New York.
Pietruszko, R., & Theorell, H. (1969) *Arch. Biochem. Biophys. 131*, 288–298.
Smith, M., Hopkinson, D. A., & Harris, H. (1973) *Ann. Hum. Genet. 37*, 49–67.
Strydom, D. J., & Vallee, B. L. (1982) *Anal. Biochem. 123*, 422–429.
Vallee, B. L., & Bazzone, T. J. (1983) in *Isoenzymes: Current Topics in Biological and Medical Research* (Scandalios, J. G., Rattazzi, M. C., & Whitt, G. S., Eds.) Vol. 8 (in press).
von Wartburg, J.-P., & Schürch, P. M. (1968) *Ann N.Y. Acad. Sci. 151*, 936–946.
Yoshida, A., Impraim, C. C., & Huang, I.-Y. (1981) *J. Biol. Chem. 256*, 12430–12436.

Self-Association of the Cardiac Fatty Acid Binding Protein. Influence on Membrane-Bound, Fatty Acid Dependent Enzymes†

Nestor C. Fournier,* Michael Zuker, Ross E. Williams, and Ian C. P. Smith

ABSTRACT: The present study on the fatty acid binding protein, purified from pig heart and studied by three independent techniques (electron spin resonance, circular dichroism, and polyacrylamide gel electrophoresis), suggests that the protein self-aggregates and exists in at least four distinct molecular species. This plurality is demonstrated by the presence of four bands after electrophoretic migration at pH 7.2 and by three transitions of molar ellipticity θ_{225} that depend on protein concentration. A mathematical model is formulated to simulate the three transitions and to calculate the concentrations of the four species. The multistates manifest themselves in a complex binding capacity for fatty acid, with two sigmoidal components in the binding curve. A general equation for the curve is formulated, and the characteristic constants are evaluated by a nonlinear least-squares fit. The experimental results and their interpretation in quantitative terms lead to a theoretical evaluation of the importance of this new property of self-aggregation of the protein on the activity of membrane-bound model enzymes which are fatty acid or acyl coenzyme A dependent.

The fatty acid binding protein, of molecular weight 12 000 (Fournier et al., 1978) and cytoplasmic origin (Capron et al., 1979; Rüstow et al., 1979), discovered some 10 years ago in most organs (Levi et al., 1969; Ockner et al., 1972), is capable of binding fatty acids, acyl coenzyme A (acyl-CoA),[1] and acylcarnitine derivatives (Mishkin & Turcotte, 1974a). Of the properties studied so far, the most remarkable is the indirect control the protein exercises on the activity of important membrane enzymes such as mitochondrial ATP/ADP translocase (Barbour & Chan, 1979), mitochondrial and microsomal acyl-CoA synthetase (Wu-Rideout et al., 1976; Ockner & Manning, 1976), or the microsomal enzymes responsible for the synthesis of phospholipids and triglycerides (O'Doherty & Kuksis, 1975; Mishkin & Turcotte, 1974b; Iritani et al., 1980; Mishkin & Roncari, 1976). This protein warrants great attention as it is the only transporter described to date which is presumably capable of translocating fatty acids and their CoA derivatives in the cytoplasm. Despite the importance of the protein and its activities, no information on the driving force or the molecular mechanism of fatty acid binding has appeared. Furthermore, what data are available on the binding isotherm are not quantitatively interpretable because of the use of an impure protein preparation (Mishkin & Turcotte, 1974a) or the lack of detailed elaboration (Ketterer et al., 1976). This is apparently due to the inapplicability of the classical technique of equilibrium dialysis for long-chain fatty acids, a consequence of the restricted diffusibility of the latter.

We report here a new property for this protein; experimental evidence obtained by three independent techniques (CD, ESR, and polyacrylamide gel electrophoresis) suggests that the fatty acid binding protein purified from cardiac muscle can self-aggregate and exist in at least four molecular states. The predictable importance of this property on the transfer of fatty acid or acyl-CoA between the cytoplasm and membranes is analzyed.

Materials and Methods

Chemicals. The spin-label 12-doxylstearic acid was purchased from Syva (Palo Alto, CA) and used as the potassium salt. Acrylamide was from Serva and Pharmalyte, pH 4–6.5, from Pharmacia.

† From the Division of Biological Sciences, National Research Council of Canada, Ottawa, Ontario, Canada K1A 0R6. *Received January 26, 1982; revised manuscript received October 28, 1982.*

* Correspondence should be addressed to this author at the Nestlé Research Department, CH-1814 La Tour-de-Peilz, Switzerland. He is the recipient of Swiss National Research Fund Grant 83.733.0.79.

[1] Abbreviations: ESR, electron spin resonance; CD, circular dichroism; 12-doxylstearic acid, 2-(10-carboxydecyl)-2-hexyl-4,4-dimethyl-3-oxyoxazolidine; acyl-CoA, acyl coenzyme A; EDTA, ethylenediaminetetraacetic acid; $NaDodSO_4$, sodium dodecyl sulfate; Temed, *N,N,N',N'*-tetramethylethylenediamine; Tris, tris(hydroxymethyl)-aminomethane.

0006-2960/83/0422-1863$01.50/0

Protein. Protein isolation from pig heart and purity control were performed according to our previously published method (Fournier et al., 1978). Before utilization, the protein was dialyzed overnight at 6 °C against a pH 7.2 buffer containing 7.9×10^{-3} M sodium phosphate, 3.97×10^{-4} M EDTA, 6.7×10^{-2} M KCl, and 0.1 M saccharose. This buffer was used in all experiments described in this paper.

ESR Spectroscopy. The binding capacity of the protein for the spin-labeled fatty acid (12-doxylstearate) was quantitatively determined by ESR, by comparison of the spectrum of the test sample with that of a standard of known fatty acid concentration, according to Hsia et al. (1973). Specific details are given under Results. Spectra were recorded at 25 ± 2 °C with a Varian E-9 spectrometer (X band), using 100-KHz field modulation.

Circular Dichroism (CD). Measurements were made on a calibrated (Gillen & Williams, 1975) Cary 61 spectropolarimeter at 25 ± 2 °C in 0.1- or 0.05-cm quartz cells. A mean residue molecular weight of 110 was used to calculate the CD parameter, θ. Determination of protein secondary structure from the CD spectra was according to the method of Provencher & Glöckner (1981), using 1-nm readings and a data set between 200 and 250 nm. Protein concentrations in milligrams per milliliter were measured according to Bradford (1976).

Polyacrylamide Gel Electrophoresis. A $NaDodSO_4$-containing gel was processed according to the method of Laemmli (1970). The isoelectric focusing gel was polymerized after being mixed in 100 mL of distilled water, 38.4 g of saccharose, 10.2 g of acrylamide, 120 mg of bis(acrylamide), 84 mg of ammonium persulfate, 88 μL of Temed, and 5 mL of Pharmalyte, pH 4–6.5; electrode solutions were 0.1 M NaOH and 0.1 M phosphoric acid. Migration took place overnight in glass tubes (length 10 cm, diameter 6 mm) at 2.5 mA/gel. The normal-type gel was polymerized after being mixed in 100 mL of distilled water, 7.36 mL of 1 N HCl, 5.57 g of Tris base, 10.26 g of acrylamide, 269 g of bis(acrylamide), and 85 mg of ammonium persulfate. A prerun of 1 h, in the absence of protein, was made at 2.5 mA/gel, with electrode buffer obtained by setting to 7.2 the pH of a 0.01 M Tris solution by addition of phosphoric acid. The second run, in the presence of protein, was performed by using the same pH 7.2 electrode buffer at 2.5 mA/gel, for the time periods indicated under the corresponding figure.

Critical Micelle Concentration (cmc) of 12-Doxylstearate. The quantitative determination of the spin-labeled fatty acid concentration, as described under Results, is valid only if the fatty acid is below its critical micelle concentration. Above this point, the resonance lines are broadened by spin-exchange and dipole–dipole interactions (Wertz & Bolton, 1972). The cmc was determined by measuring the dependence of the ESR signal amplitude on the spin probe concentration. Formation of micelles results in a sharp change in slope from a value of 1 at low concentration to less than 1 above the cmc (Figure 1).

Determination of the Relative Equilibrium Concentrations of the Four Aggregated Protein Species. As will be shown under Results, the cardiac fatty acid binding protein exists at least in four different molecular states, S_1–S_4, by self-aggregation. At equilibrium

$$S_4 \underset{c'_1}{\overset{c_1}{\rightleftharpoons}} S_3 \underset{c'_2}{\overset{c_2}{\rightleftharpoons}} S_2 \underset{c'_3}{\overset{c_3}{\rightleftharpoons}} S_1 \qquad (1)$$

Transition from one state to the next can be generated experimentally by changing the volume of the medium in order to vary the protein concentration, [P], without changing the total mass of protein. Thus, a transition can be considered as a result of the addition of a certain amount of protein (P) (considered as a ligand) to states S_i (considered as binders), so that

$$S_i + P \underset{k_{i1}}{\overset{k'_{i1}}{\rightleftharpoons}} S^*_{i+1} \qquad (2)$$

Evidence shown in Figure 5 and detailed under Results indicates that the transition of states S_i to the next state, S_{i+1}, is accompanied by changes of the secondary structure of the protein; thus, two steps, at least, must be considered to describe such transitions:

$$S_i + P \underset{k_{i1}}{\overset{k'_{i1}}{\rightleftharpoons}} S^*_{i+1} \underset{k_{i2}}{\overset{k'_{i2}}{\rightleftharpoons}} S_{i+1} \qquad (3)$$

The first step describes the formation of the new state, S^*_{i+1}, and the second step describes the isomerization of this newly generated state into a stabilized state, S_{i+1}, by reorganization of the secondary structure. The global transition process

$$S_i \underset{c_i}{\overset{c'_i}{\rightleftharpoons}} S_{i+1} \qquad (4)$$

can be characterized by the parameters c_i and c'_i which obviously must be considered as apparent rate constants. It is well-known that in such multistep models the apparent rate constants c_i and c'_i are in fact not constant but depend on the ligand concentration (Tanaka et al., 1982). Thus, their appropriate name should be apparent rate parameters. In our case (Figure 5), the transitions from state S_i to the next state, S_{i+1}, present a sigmoidal-type dependency upon the protein concentration, [P]. As is shown graphically in Figure 5, these transitions have been computer simulated, by using a purely mathematical model. The best simulations of the different transitions were obtained by stating that the apparent rate parameters, c_i and c'_i, were sigmoidally dependent upon the protein concentration, [P]

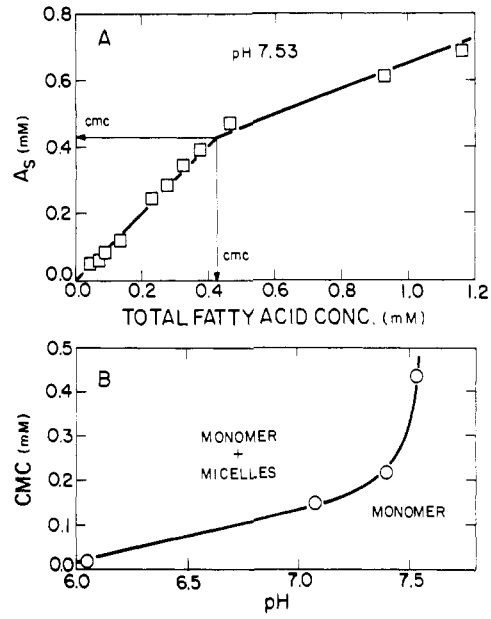

FIGURE 1: Determination of the critical micelle concentration (cmc) of 12-doxylstearate. (A) The buffer solution, containing 2.6 mM 12-doxylstearate, final pH 7.53, was heated 2 min at 100 °C; after immediate dilution in successive test tubes containing the buffer at pH 7.53, the samples were left at room temperature for 2 h. The ESR high-field line (h^{-1}) was then recorded at 25 ± 2 °C and compared quantitatively (Hsia et al., 1973) with the corresponding line of a standard pH 7.53 sample containing 0.1 mM 12-doxylstearate in the completely soluble form A_s, since the concentration was less than the cmc. (B) pH dependence of the cmc.

$$c_i = \frac{b}{1 + ([P]/a_i)^{n_i}} \qquad i = 1, 2, 3 \tag{5}$$

and by multiplicative symmetry

$$c'_i = \frac{b}{1 + (a_i/[P])^{n_i}} \tag{6}$$

When [P] (expressed in grams per liter) is increased, c_i decreases and c'_i increases so that

$$b = c_i + c'_i = \text{constant} \qquad i = 1, 2, 3 \tag{7}$$

For each transition $S_i \rightleftarrows S_{i+1}$, the a_i term in eq 5 and 6 is a mathematical constant equal to the protein concentration, [P], at which $[S_i] = [S_{i+1}]$; n_i is also a mathematical constant, related to the protein concentration $[P_i]$ at which an inflection point occurs in the sigmoidal-type transition curves. The two constants a_i and n_i are related to $[P_i]$ by the following mathematical expression:

$$[P_i] = a_i\left(\frac{n_i - 1}{n_i + 1}\right)^{1/n_i} \tag{8}$$

This very efficient, but purely mathematical, model was preferred to a classical stoichiometric model since we do not know the molecular weight or aggregation number of the four aggregated species.

After resolution of the four differential equations implicitly stated in eq 1, it is clear that at equilibrium

$$[S_1]:[S_2] = c_3:c'_3 \tag{9}$$

$$[S_2]:[S_3] = c_2:c'_2 \tag{10}$$

$$[S_3]:[S_4] = c_1:c'_1 \tag{11}$$

Thus, the equilibrium ratios of $[S_1]:[S_2]:[S_3]:[S_4]$ are respectively

$$1:\frac{c'_3}{c_3}:\frac{c'_2c'_3}{c_2c_3}:\frac{c'_1c'_2c'_3}{c_1c_2c_3}$$

To make the mathematical expression easier, we define the following auxiliary functions in which the second equalities are derived from eq 5–7:

$$F_2 = \frac{c'_3}{c_3} = \frac{[P]^{n_3}}{{a_3}^{n_3}} \tag{12}$$

$$F_3 = \frac{c'_2c'_3}{c_2c_3} = \frac{[P]^{n_3+n_2}}{{a_3}^{n_3}{a_2}^{n_2}} \tag{13}$$

$$F_4 = \frac{c'_1c'_2c'_3}{c_1c_2c_3} = \frac{[P]^{n_3+n_2+n_1}}{{a_3}^{n_3}{a_2}^{n_2}{a_1}^{n_1}} \tag{14}$$

We further define $F_1 = 1$ and $F = F_1 + F_2 + F_3 + F_4$. The concentrations of the respective molecular species are then

$$[S_1] = \frac{[P]F_1}{F} \tag{15}$$

$$[S_2] = \frac{[P]F_2}{F} \tag{16}$$

$$[S_3] = \frac{[P]F_3}{F} \tag{17}$$

$$[S_4] = \frac{[P]F_4}{F} \tag{18}$$

These concentrations can be expressed either in percent or in true concentration values.

If the transitions between the different states induced by successive dilution of the protein, P, in the medium can be monitored by biophysical measurements (in our case, by monitoring the change of the ellipticity, θ, at 225 nm by circular dichroism; Figure 5), the unknown parameters n_1, n_2, and n_3 and a_1, a_2, and a_3 in eq 12–14, and required to solve eq 15–18, can be estimated (Table I).

Table I: Computer-Estimated Values[a] of the Parameters a_i and n_i Required in Equations 12–18 for the Determination of the Concentration of the Four Molecular Species S_1–S_4 (Figures 7 and 8)

parameter	value	parameter	value
a_1	2.00 ± 0.14	a'_1	1.84 ± 0.09
a_2	1.16 ± 0.23	a'_2	2.08 ± 0.16
a_3	0.69 ± 2.10	a'_3	0.77 ± 1.90
n_1	50 ± 28	n'_1	42 ± 24
n_2	18 ± 15	n'_2	2 ± 2.3
n_3	(26 ± 15) × 10^5	n'_3	(56 ± 13) × 10^4

[a] The parameters and their corresponding standard errors were calculated from experimental data (Figure 5) according to the mathematical procedure described under Materials and Methods. a_i and a'_i terms are given in grams per liter; a_3 and a'_3 correspond to the protein concentration at which $[S_1] = [S_2]$; a_2 and a'_2 correspond to the concentration at which $[S_2] = [S_3]$; a_1 and a'_1 correspond to the concentration at which $[S_3] = [S_4]$. n_i values are constant terms characterizing the slope of the transition from one state, S_i, to the next state, S_{i+1}, as specified in eq 5, 6, and 8. a_1–a_3 and n_1–n_3 refer to the protein in pH 7.2 buffer, whereas a'_1–a'_3 and n'_1–n'_3 refer to the protein in pH 7.2 buffer containing 0.325 × 10^{-4} M potassium stearate.

This estimation is performed by introducing four new parameters: θ_1, θ_2, θ_3, and θ_4. They correspond to the ellipticities, θ_{225nm}, of the four species S_1, S_2, S_3, and S_4, respectively. From the discussion above, it is clear that

$$\theta = \sum_{i=1}^{4}\frac{\theta_i F_i}{F}$$

should correspond to the experimentally observed ellipticity at 225 nm and the protein concentration, [P]. If θ_j values (where $j = 1, \ldots, m$) are m observed ellipticities at protein concentrations $[P_j]$ (where $j = 1, \ldots, m$), then the ten parameters θ_1, θ_2, θ_3, θ_4, a_1, a_2, a_3, n_1, n_2, and n_3 are estimated by varying them so that the quantity

$$\sum_{j=1}^{m}\left(\theta_j - \sum_{i=1}^{4}\frac{\theta_i F_{ji}}{F_j}\right)^2$$

is minimized.

This nonlinear least-squares problem is solved by using Marquardt's algorithm (Marquardt, 1963) which yields not only the estimated parameters a_1, a_2, a_3, n_1, n_2, and n_3 but also the estimated values of θ_1–θ_4.

Results

Binding of Fatty Acid to the Protein. The binding capacity, $\bar{v}$, is defined by the ratio $[A_b]:[P]$, where $[A_b]$ is the number of moles of fatty acid bound per gram of protein P. To facilitate the quantitative determination of $[A_b]$, we have chosen 12-doxyl spin-labeled stearic acid as a ligand. The paramagnetic nitroxide moiety yields a simple three-line ESR spectrum when the fatty acid is free in the medium and rotating rapidly and isotropically (Figure 2A,B). The immobilization of the fatty acid on binding to the protein leads to strong broadening of the resonances, particularly that at high field, h^{-1}, where amplitude becomes virtually undetectable (Figure 2A′). When the ratio of spin-labeled fatty acid to protein is increased, the ESR spectrum (Figure 2B′) contains two subspectra, indicative of the spin probe bound to protein

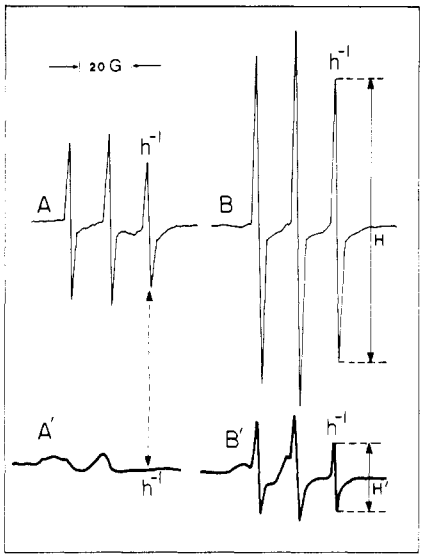

FIGURE 2: Fatty acid binding to the protein as visualized by ESR. (A) Calibration sample containing the pH 7.4 buffer plus 3.1 μM 12-doxylstearate. (A') Same as in (A) plus protein; the molar ratio of fatty acid:protein is 0.016. (B) Same as in (A) but with 8.5 μM 12-doxylstearate. (B') Same as in (B) plus protein; the molar ratio of fatty acid:protein is 0.048. Spectra were obtained with the same instrument gain: 5×10^3 for (A) and (A'); 4×10^3 for (B) and (B').

and free in solution, with slow exchange (on the ESR time scale) between the two sites. Resonance h^{-1} contains a negligible contribution from the subspectrum due to the bound probe, and hence is a measure of $[A_s]$. If we define $[A_{st}]$ as the known concentration of spin-labeled fatty acid in a standard solution, the concentration of probe free in the medium of the protein-containing solution, $[A_s]$, may be calculated from $[A_{st}]/[A_s] = H/H'$, in which H and H' (Figure 2) are the amplitudes of resonance h^{-1} in the two solutions. The simple amplitudes of the first-derivative spectra may be employed because, at constant temperature, the line shapes of the spectra are identical in both samples. The concentration of bound probe, $[A_b]$, is given by the difference $[A_{st} - A_s]$, and the binding capacity, $\bar{\nu}$, is then calculated from the ratio $[A_b]:[P]$.

The $\bar{\nu}$ variations were analyzed as a function of the variables $[A_s]$ and [P]. The binding curve (Figure 3) is complex, exhibiting two important slope changes at protein concentrations about equal to 2 and 0.8 g L^{-1}. The curve is unusual since at high equilibrium fatty acid concentration ($[A_s] > 30$ μM), the binding capacity, $\bar{\nu}$, does not reach a plateau but decreases.

The initial part of the experimental binding curve was deconvoluted by a nonlinear least-squares fit into one hyperbolic and two sigmoidal functions (Figure 3, curves I–III). Thereby, the binding capacity curve can be described by the following analytical expression for $[A_s]$ values less than 30 μM:

$$\bar{\nu} = \frac{[A_b]}{[P]} = \frac{\bar{\nu}_{max\ I}}{1 + K_I/[A_s]} + \frac{\bar{\nu}_{max\ II}}{1 + (K_{II}/[A_s])^{n_{II}}} + \frac{\bar{\nu}_{max\ III}}{1 + (K_{III}/[A_s])^{n_{III}}} \quad (19)$$

$[A_b]$, $[A_s]$, and [P] are the variables defined previously; K_i values are the points of half-saturation of curves I–III (the $[A_s]$ at which $\bar{\nu} = \bar{\nu}_{max}/2$); n_i values determine the concentration, $[A_{si}]$, at which the inflection points occur on the sigmoidal curves:

$$[A_{si}] = K_i\left(\frac{n_i - 1}{n_i + 1}\right)^{1/n_i} \quad (20)$$

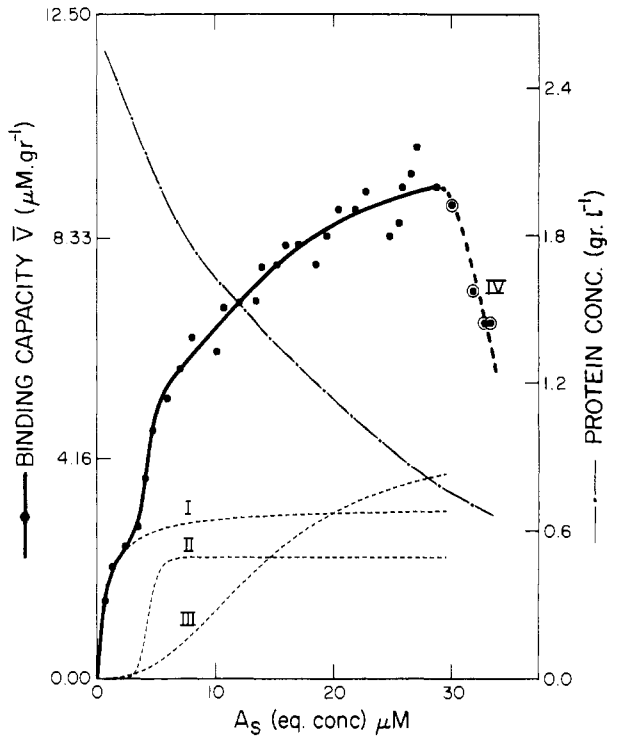

FIGURE 3: Binding capacity of 12-doxylstearate to the protein. The protein, initially 2.82 g L^{-1} in pH 7.2 buffer at 25 ± 2 °C, was progressively diluted with a stock solution containing 0.05 mM doxylstearate in the same buffer. At each dilution step, the free fatty acid equilibrium concentration, $[A_s]$, and the protein-bound fatty acid concentrations, $[A_b]$, were quantitatively determined by ESR (Hsia et al., 1973) as described under Results. Thereby, the binding capacity, $\bar{\nu}$, was calculated from the ratio $[A_b]:[P]$, where [P] is the protein concentration in grams per liter. The solid line represents the theoretical binding curve obtained by computer simulation according to eq 19 and the parameters of Table II and fitted to the experimental points for $[A_s]$ values <30 μM; the dashed lines represent the computer deconvolution of this initial part of the binding curve into the three following primary functions: one hyperbolic curve (I) and two sigmoidal curves (II and III). The experimental points (⊙) obtained for $[A_s] > 30$ μM were not used in the computer-fitting process, since no easily tractable function was found to be added to the initial functions. (–·–) represents the protein concentration.

Table II: Computer-Determined Values[a] according to Equation 19 and Experimental Points (Figure 3) of the Constants Characterizing the Binding Capacity of 12-Doxylstearate to the Protein

parameter	value (μM g^{-1})	parameter	value (μM L^{-1})
$\bar{\nu}_{max\ I}$	3.25 ± 1.33	K_I	0.85 ± 0.89
$\bar{\nu}_{max\ II}$	2.33 ± 1.25	K_{II}	4.38 ± 0.35 (n_{II}, 10.1 ± 8.6)
$\bar{\nu}_{max\ III}$	4.50 ± 2.42	K_{III}	14.4 ± 2.3 (n_{III}, 2.6 ± 1.8)

[a] The parameters and their corresponding standard errors were estimated by nonlinear least-squares regression using a Gauss–Newton algorithm. $\bar{\nu}_{max\ I}$ characterizes the maximum binding capacity in the hyperbolic part of the binding curve (Figure 3, curve I); $\bar{\nu}_{max\ II}$ and $\bar{\nu}_{max\ III}$ characterize the two sigmoidal parts (Figure 3, curves II and III); K values are equal to free fatty acid equilibrium concentrations, $[A_s]$, for which the binding capacity, $\bar{\nu}$, is equal to half-maximum in curves I–III (Figure 3); n_{II} and n_{III} are parameters defining the inflection points in curves II and III, respectively, as specified under Results (eq 20).

The numerical values of $\bar{\nu}_{max\ i}$, K_i, and n_i in eq 19 were determined by computer and reported in Table II with their corresponding standard errors.

Several molecular events can take place when a small ligand interacts with a macromolecule. The ligand can induce a conformational change of the protein, new binding sites thus

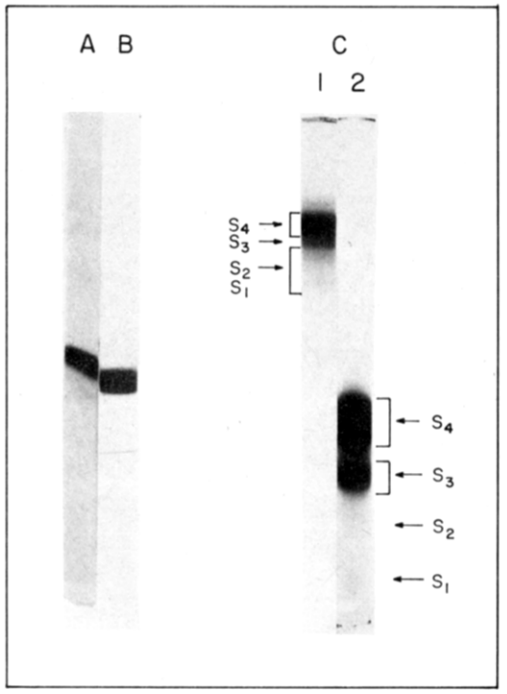

FIGURE 4: Polyacrylamide gel electrophoresis of the purified protein. (A) Isoelectric focusing in a gel containing Pharmalyte, pH 4–6.5; protein amount, 380 μg. (B) $NaDodSO_4$ gel; protein amount, 67 μg. (C) pH 7.2 Tris–phosphoric acid gel; protein amount, 326 μg: (1) migration time, 3 h; (2) migration time, 8.5 h, 2.5 mA/gel.

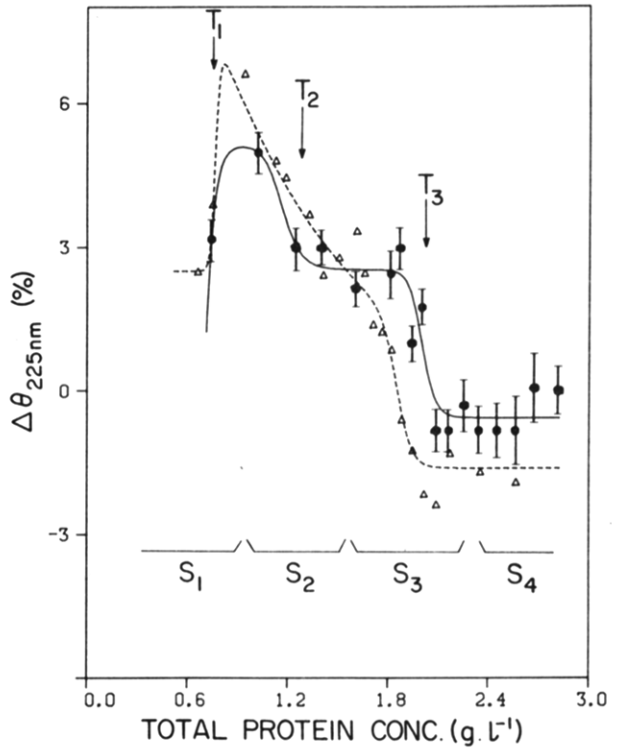

FIGURE 5: Variation of the ellipticity at θ_{225nm} with protein concentration. Successive dilutions of the protein were performed by adding pH 7.2 buffer (●) or pH 7.2 buffer containing 0.325×10^{-4} M potassium stearate (△); the θ_{225nm} reference value was determined at a protein concentration equal to 2.82 g L^{-1}. The solid and dashed lines are computer-simulated curves obtained by fitting the theoretical model developed under Materials and Methods to the experimental points. Transitions are indicated by T_1, T_2, and T_3 and suggested protein states by S_1, S_2, S_3, and S_4. Vertical bars indicate the variations observed for two series of measurements.

becoming available and the slope of the binding curve changing dramatically. This ligand-induced conformational change of the protein can also modify the affinity of fatty acid for some binding sites, leading to a leak of the bound fatty acid from the protein. In the latter case, the absence of a plateau in the curve is expected. Furthermore, our experimental procedure to determine the binding capacity was designed in such a way as to allow a progressive decrease of the protein concentration in the sample (Figure 3); thus, the probability of protein–protein interactions, for example, by self-aggregation, will also decrease. If we suppose that fatty acid binds preferentially to high molecular weight self-aggregated protein molecules and does not bind or poorly binds to the monomeric protein, the absence of a plateau but the appearance of decreasing values of the binding capacity to fatty acid, when the protein is diluted, is also predictable.

The following part of our work was undertaken to discriminate which of the above-mentioned parameters are responsible for this unusual binding curve.

Analysis of the Electrophoretic Properties of the Protein. Electrophoresis of the protein in polyacrylamide gels (Weber & Osborn, 1969), preequilibrated at pH 7.2, was characterized by the appearance of a large and diffused protein band when the migration time was short (Figure $4C_1$); when the time was increased, this diffused band segregated into four bands, S_1–S_4, the fast migrating species being the least intense (Figure $4C_2$). This pattern suggests the coexistence of different molecular weight protein species. This heterogeneity cannot be due to an impure preparation since in the $NaDodSO_4$-type gel (Figure 4B) and in the isoelectric focusing type gel Figure 4A) clearly a unique band was detected characterized by a molecular weight of about 12000, as determined by comparison with the standard protein and by a p*I* of 4.8 ● 0.03. Consequently, it is suggested that the pure protein gives rise to multi molecular weight species by self-aggregation. The lack of clear-cut resolution of the bands (Figure 4C) could be due to a rapid reequilibration between the different species generated by the diffusion gradient of the protein, when the latter migrates in the electric field.

Analysis of the Protein by Circular Dichroism. The possibility of self-aggregation of the protein, as suggested above, was tested by circular dichroism analysis. If a protein exists only as a monomeric unit, no variation of the molar ellipticity, θ, is expected, when measured at a fixed wavelength and a given protein concentration. On the contrary, if self-aggregation takes place, the protein molecules collide, and in the domain of anchorage, some structural changes are predictable and indicated by modifications of the molar ellipticity θ of the protein.

Such variations were effectively observed by measuring the variations of molar ellipticity, $\Delta\theta$, at 225 nm, whereas the protein was diluted progressively from 2.82 to 0.6 g L^{-1}. In this concentration range, three transitions, T_1, T_2, and T_3, of θ values were observed respectively at about 0.8, 1.2, and 2 g L^{-1} (Figure 5). Basically the same transitions were observed in the absence as well as in the presence of fatty acid (Figure 5). These transitions take place at the same protein concentration at which the binding capacity curve of fatty acid to protein dramatically changes its slope (Figure 3). Thus, this correlation between the changes in the protein state and the changes in the binding capacity of fatty acid to the protein suggests that the former induces the latter.

These structural changes concern the α, the random coil, and the β-turn secondary structures but not the β structure. Analyses of the wavelength dependence (190–300 nm) of the molar ellipticity (θ) of the protein allow quantification of the relative contributions of these four secondary structure components (Provencher & Glöckner, 1981; Chen et al., 1974).

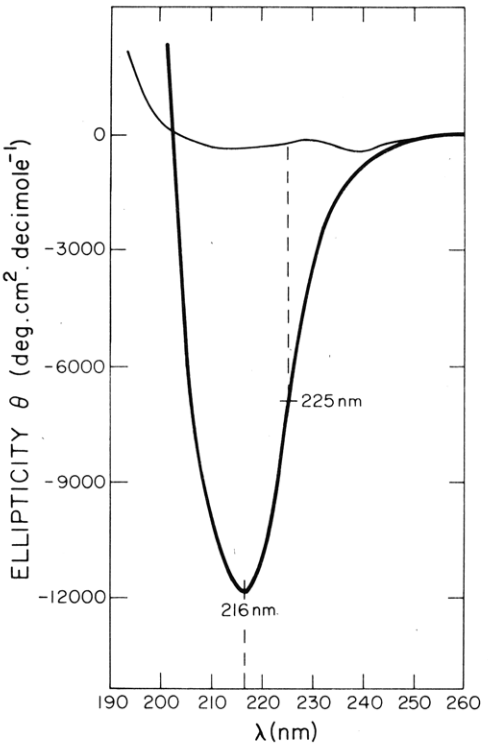

FIGURE 6: Circular dichroism spectrum of the protein. Protein concentration was 2.82 g L^{-1} in pH 7.2 buffer.

The CD spectrum of the protein has a minimum at 216 nm (Figure 6); this is typical of a protein rich in β structure. The contributions of the four types of secondary structure calculated by computer from the experimental spectra according to Provencher & Glöckner (1981) at high (2.82 g L^{-1}) and low (0.6 g/L^{-1}) protein concentrations, respectively, were the following: β, 48%, 48%; α, 26%, 19%; random coil, 22%, 25%; β turn, 4%, 8%. This concentration dependency would not be observed if the protein was monomeric.

The three transitions T_1–T_3 observed between 0.6 and 2.82 g L^{-1} (Figure 5) suggest the existence of at least four molecular species which we designate as S_1–S_4 (Figure 5). These three transitions, T_1–T_3, and the relative equilibrium concentration of species S_2–S_4, have been simulated and calculated by solving eq 12–18 after determination of the constants a_i and n_i (Table I) from the experimental data (Figure 5), by means of the formalism described under Materials and Methods. A good fit of the simulated curves to the experimental points can be observed in Figure 5. However, the transition T_1 corresponding to the formation of protein species S_1 is poorly defined, as indicated by the large standard error of the parameters a_3, a'_3, n_3, and n'_3 in Table I. Thus, only the relative equilibrium concentrations of species S_2, S_3, and S_4 have been computerized and plotted in Figures 7 and 8.

In the absence of stearic acid, species S_2 and S_3 are coexisting when the total protein concentration is between 0.83 and 1.62 g L^{-1} and protein species S_3 and S_4 when the concentration is between 1.73 and 2.28 g L^{-1} (Figure 7). The presence of stearic acid modifies dramatically the distribution of these protein species; the coexistence of the three protein species S_2, S_3, and S_4 is observed for a total protein concentration of 1.58–2.4 g L^{-1} (Figure 8).

The significant influence of stearic acid on the protein species distribution, as visualized by comparison of Figures 7 and 8, suggests that the processes of protein aggregation and fatty acid binding to the protein involve common binding sites on the protein molecule and are thus competitive processes.

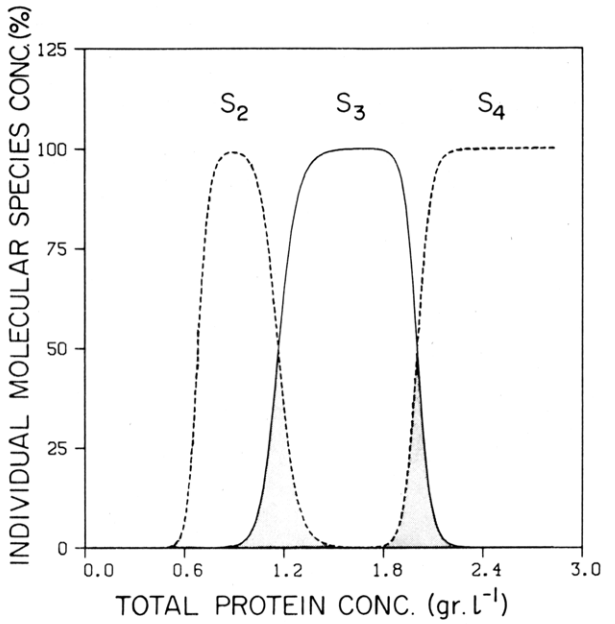

FIGURE 7: Molecular species distribution as a function of protein concentration in pH 7.2 buffer. The respective concentrations of states S_2, S_3, and S_4 were calculated by solving eq 12–18 after determination of the constants a_i and n_i (Table I) from experimental data (Figure 5) and by using the mathematical formalism described under Materials and Methods.

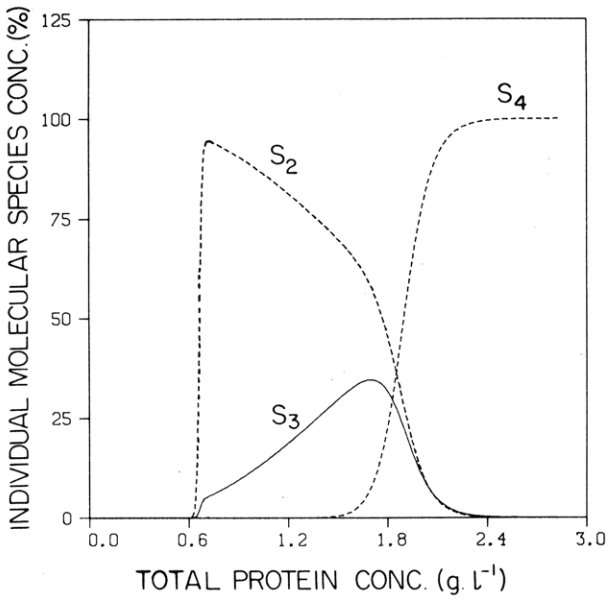

FIGURE 8: Molecular species distribution as a function of protein concentration in pH 7.2 buffer containing 0.325×10^{-4} M potassium stearate. The procedure was described in the legend for Figure 7.

Predictable Influence of the Self-Associated Nature of the Cytoplasmic Fatty Acid Binding Protein on the Performance of Fatty Acid (or Acyl-CoA) Dependent Enzymes Bound to a Model Membrane. Enzymes which are membrane bound and fatty acid dependent, such as mitochondrial or microsomal acyl-CoA synthetases, have been observed to be strongly controllable by the cytoplasmic fatty acid binding protein (Wu-Rideout et al., 1976; Ockner & Manning, 1976; Burnett et al., 1979). The latter binds equally well to acyl-CoA (Mishkin & Turcotte, 1974a). Thus, it is not surprising that an efficient control by this protein was also observed on acyl-CoA-dependent enzymes bound to membranes, such as the microsomal triglyceride synthetase (O'Doherty & Kuksis, 1975; Iritani et al., 1980) or the phospholipid synthetases

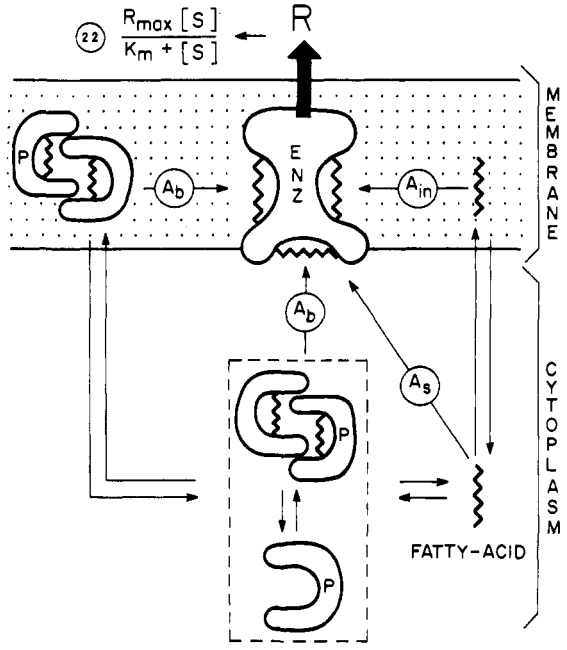

FIGURE 9: Model for the interaction of the fatty acid or acyl-CoA binding protein (P) with a membrane enzyme (ENZ) whose activity depends upon the supply of these substrates. The symbols A_{in}, A_s, and A_b represent fatty acid or acyl-CoA solubilized in the membrane, free in the cytoplasm, and bound to the protein, respectively. The protein may exist in several states of aggregation, of which the monomeric state cannot bind the substrate. The response of the enzyme is of the Michaelis–Menten type, as described by eq 22.

(Mishkin & Turcotte, 1974b; Mishkin & Roncari, 1976; Burnett et al., 1979).

This regulation is quite important, due to its position at the beginning of the metabolic pathways for degradation and synthesis of lipids. The type of control exercised by this cytoplasmic protein on the membrane-bound enzyme activity can be either stimulation (Wu-Rideout et al., 1976; Ockner & Manning, 1976; O'Doherty & Kuksis, 1975; Mishkin & Turcotte, 1974b; Iritani et al., 1980; Mishkin & Roncari, 1976), inhibition (Wu-Rideout et al., 1976; Mishkin & Roncari, 1976), or modulation (Burnett et al., 1979; Fournier, 1978), depending on the enzyme considered. No mechanism has been proposed to date which explains these three different modes of regulation. The following model is dedicated to this problem.

A fatty acid dependent or acyl-CoA-dependent enzyme, E, is considered to be bound to a membrane, M (Figure 9). We assume that fatty acid (or acyl-CoA) can exist in a soluble state A_s, free in the medium and in equilibrium with the species A_{in}, which is solubilized in the lipid domains in the membrane and also in equilibrium with the species A_b, which is bound to the protein P in the medium (Figure 9).

The model requires determination of the partition coefficient, p, of fatty acid or acyl-CoA between the two states A_s and A_{in}. An estimate was made for isolated cardiac mitochondria, by using the spin probe 12-doxylstearic acid. The equilibrium concentrations $[A_s]$ and $[A_{in}]$ were determined by measurement of the amplitudes of the resonance lines at high field, h^{-1}, and by comparison with a standard as described previously. The ratio $[A_{in}]/[A_s]$ was observed to vary linearly with the concentration of mitochondria (protein concentration <2 g L^{-1}) according to the following:

$$\frac{[A_{in}]}{[A_s]} = p[M] \tag{21}$$

in which p represents the partition coefficient in liters per gram of protein and [M] is the concentration of mitochondria in grams of protein per liter. The value of p, determined by linear regression, is 3.55. The value of [M] in the model was taken arbitrarily as 1 g of protein L^{-1}. Furthermore, we assume that the dependence of the enzyme activity rate, R, on the fatty acid or acyl-CoA substrate concentration, [S], is of the Michaelis–Menten type:

$$R = \frac{R_{max}[S]}{K_m + [S]} \tag{22}$$

The following arbitrarily chosen values have been assigned: $R_{max} = 5.08 \times 10^{-4}$ M min^{-1} (g of protein)$^{-1}$; $K_m = 2.5 \times 10^{-4}$ M. Defining $[A_t]$ as the total concentration of fatty acid or acyl-CoA in the system:

$$[A_t] = [A_{in}] + [A_s] + [A_b] \tag{23}$$

which from eq 19 and 21 become

$$[A_t] = p[A_s][M] + [A_s] + [P]\left[\frac{\bar{v}_{max\,I}}{1 + K_I/[A_s]} + \frac{\bar{v}_{max\,II}}{1 + (K_{II}/[A_s])^{n_{II}}} + \frac{\bar{v}_{max\,III}}{1 + (K_{III}/[A_s])^{n_{III}}}\right] \tag{24}$$

$[A_t]$ was arbitrarily set equal to 1×10^{-4} M. The numerical values of constants, $\bar{v}_{max\,i}$, K_i, and n_i, required in eq 24 are reported in Table II. Computer simulations of enzyme performance as a function of the type of substrate S introduced in eq 22 are analyzed.

In the first case, fatty acid or acyl-CoA, A_b, bound to the protein P, is considered as the source of substrate S required by the enzyme. We assume that the protein may transfer fatty acid or acyl-CoA to the enzyme by direct close-contact interaction at the surface of the membrane or after integration of the protein–fatty acid complex into the membrane (Figure 9). The protein P, as suggested under Results, can exist after self-aggregation, at least under four different molecular species, S_1–S_4. If it is assumed that the three active protein species S_2, S_3, and S_4 are all able to transfer fatty acid or acyl-CoA to the enzyme, an explicit value of $[A_b]$, as a function of the protein concentration [P], can be obtained after extraction of $[A_s]$ from eq 24 and then substitution into eq 19, finally followed by substitution of [S], in eq 22, by this explicit value of $[A_b]$.

A linear increase of the enzyme activity is observed (Figure 10a) when the concentration of the protein is increased. However, if we assume that selectivity only one among the active species, S_2, S_3, or S_4, is able to transfer fatty acid or acyl-CoA to the enzyme, a strong modulation of the enzyme activity is observed when the concentration of protein P is varied in the sample. Figure 10b,c shows the modulation observed when the protein species considered are either S_3 or S_4, with their corresponding fatty acid or acyl-CoA bound species, respectively, A_{bs3} or A_{bs4}. The explicit values of $[A_{bs3}]$ and $[A_{bs4}]$ as a function of the protein concentration [P] were obtained from the following:

$$[A_b] = [P]\bar{v} = \bar{v}([S_1] + [S_2] + [S_3] + [S_4]) \tag{25}$$

$$[A_{bs3}] = \bar{v}[S_3] \tag{26}$$

$$[A_{bs4}] = \bar{v}[S_4] \tag{27}$$

An explicit value of $\bar{v}$ is obtained by extracting $[A_s]$ from eq 24 and substituting it in eq 19. Explicit values of $[S_3]$ and $[S_4]$ as a function of [P] are obtained by substitution of the n_i and a_i parameters in eq 13 and 14 with their numerical

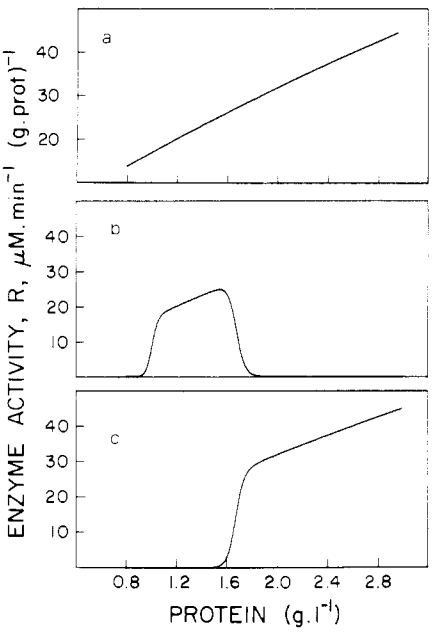

FIGURE 10: Computer simulation (described under Results) of the activity of a model enzyme bound to a membrane (Figure 9) and requiring fatty acid or acyl-CoA as substrate. These substrates are given up to the enzyme by the cytoplasmic fatty acid or acyl-CoA binding protein, which is assumed to exist in four different molecular states (S_1–S_4) by self-aggregation. The transfer of substrate from the cytoplasm to the membrane-bound enzyme is assumed to be performed (a) simultaneously by the three active species S_2, S_3, and S_4, (b) only by the species S_3, or (c) only by the species S_4. On the abscissa, the term "protein" refers to the total protein concentration ($[S_1] + [S_2] + [S_3] + [S_4]$). The total fatty acid or acyl-CoA concentration in the medium was assumed to be equal to 1×10^{-4} M.

values, reported in Table I. This operation gives rise to explicit values of F_3 and F_4, in eq 13 and 14. These latter values are finally introduced respectively in eq 17 and 18, and the resulting explicit values of $[S_3]$ and $[S_4]$ are substituted respectively in eq 26 and 27. As a final result, $[A_{bs3}]$ and $[A_{bs4}]$ are explicit with respect to [P] and thus can be substituted for [S] in eq 22.

In the second case, fatty acid or acyl-CoA free (A_s) in the medium, or present (A_{in}) in the lipid part of the membrane (Figure 9), was successively considered as substrate S in eq 22. A_s substrate is assumed to reach the enzyme by direct exchange at the surface of the membrane and substrate A_{in} by lateral diffusion in the core of the membrane. An explicit value of $[A_s]$, as a function of the protein concentration [P], is obtained by extraction of $[A_s]$ from eq 24. An explicit value of $[A_{in}]$ can be defined by extracting $[A_s]$ from eq 24 and substituting it into eq 21. These two explicit expressions for $[A_s]$ and $[A_{in}]$ are then successively substituted for [S] in eq 22.

The results obtained (not shown) indicate, in both cases, that increasing the protein concentration depressed linearly the enzyme activity in the membrane.

In summary, although the total quantity of substrate, $[A_t]$ (fatty acid or acyl-CoA), available to the enzyme is kept constant in the analyzed system, the rate of the membrane-bound enzyme activity is strongly controllable by the concentration of the cytoplasmic fatty acid of acyl-CoA carrier. A linear or modulated dependency is observed, depending on the course followed by these two types of substrates to reach the enzyme in the membrane.

This modulation is a direct consequence of the multiaggregated nature of the protein and requires only small variations of the concentration of the protein to induce very large modifications of the enzyme activity (Figure 10b,c).

Discussion

The major conclusion emerging from the present study attributes multiple aggregation states to the cardiac fatty acid binding protein. As an essential preliminary operation, the purity of the protein has been confirmed by the fact that only a single electrophoretic band is obtained in conditions of protein overcharge on an $NaDodSO_4$-type gel (Figure 4B) and also on an isoelectric focusing type gel (Figure 4A). This criterion of purity is fully justified because the two electrophoretic techniques used discriminate the proteins as a function of two completely different parameters, i.e., mass or charge, respectively. The migration within a normal-type gel (no $NaDodSO_4$ and no pH gradient) enables us to simultaneously express the charge and mass properties of the protein. Under these conditions, at pH 7.2, the fatty acid binding protein segregates into four electrophoretic bands after migrating in a weak electric field (2.5 mA) for 8 h (Figure $4C_2$). Such an electrophoretic pattern is expected if the existence of the multiaggregated species of the protein in rapid reequilibration is supposed; $NaDodSO_4$ disaggregates these multimolecular buildings and releases the 12000-dalton monomer.

More specific intramolecular experiments were performed to verify the above suggestion. Thus, circular dichroism observations of the protein were obtained. It is obvious that, if a protein is monomeric over all its concentration range, the molar ellipticity θ, measured at a fixed wavelength, is not expected to change but should remain constant whatever the protein concentration is. With the fatty acid binding protein, changes were observed. A progressive shift of the concentration was induced by diluting the protein from 3 to 0.6 g L^{-1}. The parameter θ_{225nm} was calculated on the basis of CD spectra which were successively recorded during this dilution process. Significant and reproducible variations of θ_{225nm} were observed. Three sigmoidal-type transitions (Figure 5, T_1–T_3) took place. This suggests successive transformation of the protein into four different species, i.e., S_1–S_4. The respective concentrations of these different species were calculated by using the mathematical model described under Materials and Methods. However, the determination of S_1 concentration was not tractable since the parameters a_3, a'_3, n_3, and n'_3 of Table I, required for this determination, are poorly defined with large standard errors. The distribution of the three determined states, S_2, S_3, and S_4, vs. the total protein concentration was highly modified by the presence of fatty acid (compare Figure 8 to Figure 7). Competition for the same binding site on the protein surface between the self-aggregation process and the fatty acid binding process is thus suggested. As a consequence, we can state that both protein and fatty acid concentrations in the medium act as driving forces to generate and modulate the different aggregation states of the protein. Such a regulation is likely active in vivo and might well be very important for the intracellular distribution of fatty acids controlled by this cytoplasmic carrier.

Evidence suggesting multiaggregated states of the protein was also yielded by the determination of the binding capacity of stearic acid to the protein. This operation requires the quantitative determination of the free equilibrium concentration of fatty acid, $[A_s]$, in the medium, as well as the protein-bound fatty acid concentration, $[A_b]$. Thus, the relation $\bar{v} = [A_b]/[P] = f([A_s])$ can be established where [P] is the protein concentration. This determination is not trivial for fatty acids; the classical equilibrium dialysis method is useless, since fatty acids diffuse very slowly through the dialysis

membranes. In the present study, the elegant spin-labeling technique, using 12-doxyl spin-labeled stearic acid, was applied efficiently to these quantitative determinations. The main feature of the binding curve is the absence of a plateau at saturating concentrations of free fatty acid; instead, a decrease of the $\bar{v}$ value is observed (Figure 3). The onset of this decrease takes place for a protein concentration equal to about 0.8 g L^{-1}, corresponding to the range of concentrations where the onset of the T_1 transition was observed in the previous CD analysis (Figure 5). This unusual absence of a plateau is explainable if multiaggregated states of the protein are suggested, each of them having a differential binding capacity and the low molecular weight species having no or poor binding capacity to fatty acids.

If the protein concentration is high (>2 g L^{-1}), basically only the S_4 species is to be found (Figure 8). In this range of concentrations, the curve representing the binding capacity of stearic acid to the protein is a hyperbola (Figure 3). Thus, in this state, the protein has either only one binding site or several sites that are all equivalent. At a protein concentration of about 2 g L^{-1}, transition T_3 begins (Figure 5). The protein goes from state S_4 to S_3. The curve representing the fatty acid binding capacity to the protein undergoes a marked transition and changes from a hyperbolic shape to a sigmoidal shape in the protein concentration range between 2 and 0.8 g L^{-1} (Figure 3); in this range, several molecular protein species coexist (Figure 8), and the sigmoidal shape of the binding curve is a manifestation of this plurality. This is in agreement with the theoretical model of Nichol et al. (1967), where sigmoidal curves were also produced where a ligand binds simultaneously to several molecular species of a multiaggregated protein.

The excellent correlation between the onset of T_3 and T_1 transitions, as observed by CD analysis (Figure 5), and the change of slope in the binding capacity curve at the same protein concentration, respectively 2 and 0.8 g L^{-1} (Figure 3), obviously means that a dramatic change of the molecular properties of the protein takes place. These two changes cannot be considered fortuitous since two independent techniques detect the same phenomenon.

Important metabolic implications follow from this new self-aggregation property of the fatty acid carrier. The activity of fatty acid dependent or acyl-CoA-dependent enzymes bound to membranes was shown in the theoretical model analyzed in the present paper to be strongly regulated by the concentration of this protein. A linear or modulated dependency of the enzyme activity was observed (Figure 10), depending on the course followed by the above substrates to reach the enzymes in the membrane. This type of regulation requires fluctuations of concentrations of this protein outside but close to the membranes. This requirement is likely to be fulfilled in vivo, since this protein is inducible; a diet rich in fat was observed (Ockner & Manning, 1974) to be able to increase very significantly the total concentration of the protein. This type of regulation can be named long-term regulation.

However, in vivo, very short-term regulation can be predicted. Capron et al. (1979) have shown by immunocytochemical techniques that the protein does not have a uniform distribution in liver cells, but instead has rather a gradient-like distribution, with a preferential localization around the mitochondria and the smooth endoplasmic reticulum. The dynamics of formation of these intracellular gradients are unknown, but obviously they act as driving forces for the creation of multiaggregated states of the protein. Furthermore, the equilibrium rate between these different states is fast as suggested by the lack of a clear-cut separation between them when they migrate in electrophoresis gels (Figure 4C). Consequently, because of the existence of these rapidly fluctuating gradients, local, transient, and short-lived fluctuations of concentration of each individual self-aggregated species of the protein close to the intracellular membranes are predictable. In this situation, our theoretical model predicts a strong modulation of enzyme activity when only one of these aggregated species selectively transfers fatty acid or acyl-CoA to the dependent enzyme in the membrane (Figure 10b,c). This type of regulation can be named short-term regulation and might be effective, for example, at each cardiac pulse.

In summation, the experimental data presented here suggest that the cardiac fatty acid binding protein of molecular weight 12 000 can also exist at least under three other molecular weight forms, by self-aggregation. A rapid equilibrium might exist between the different species. The aggregation process induces small but detectable variations of secondary structures of the protein, and this process is in competition with the binding process of fatty acids to the protein. Molecular characteristics such as molecular weights and association constants of the protein species remain to be established. The theoretical analysis developed here suggests that this self-aggregation property of the fatty acid carrier might well be a powerful intracellular tool to regulate membrane-bound enzyme activity.

The projection of this model on the regulation of the β-oxidative system of heart mitochondria would be quite stimulating, since 80% of the cardiac energy is delivered through this pathway and since this fatty acid carrier protein is the unique intracellular protein described to date (Fournier et al., 1978) able to provide fatty acids as substrate to this important energy-producing system.

Acknowledgments

We thank L. Bramall for her excellent assistance with computer simulations.

Registry No. 12-Doxylstearic acid, 29545-47-9.

References

Barbour, R. L., & Chan, S. H. P. (1979) *Biochem. Biophys. Res. Commun. 89*, 1168–1177.

Bradford, M. (1976) *Anal. Biochem. 72*, 248–251.

Burnett, D. A., Lysenko, N., Manning, J. A., & Ockner, R. K. (1979) *Gastroenterology 77*, 241–249.

Capron, F., Coltoff-Schiller, B., Johnson, A. B., Fleischner, G. M., & Goldfisher, S. (1979) *J. Histochem. Cytochem. 27*, 961–966.

Chen, Y. H., Yang, J. T., & Chan, K. H. (1974) *Biochemistry 13*, 3350–3359.

Fournier, N. C. (1978) Thesis No. 1880, Faculté des Sciences, Université de Genève, Switzerland.

Fournier, N. C., Geoffroy, M., & Deshusses, J. (1978) *Biochim. Biophys. Acta 533*, 457–464.

Gillen, M. F., & Williams, R. E. (1975) *Can. J. Chem. 53*, 2351–2353.

Hsia, J. C., Wong, L. T. C., & Kalow, W. (1973) *J. Immunol. Methods 3*, 17–24.

Iritani, N., Fukuda, E., & Inoguchi, K. (1980) *J. Nutr. Sci. Vitaminol. 26*, 271–277.

Ketterer, B., Tipping, E., Hackney, J. F., & Beale, D. (1976) *Biochem. J. 155*, 511–521.

Laemmli, U. K. (1970) *Nature (London) 227*, 680–685.

Levi, A. J., Gatmaitan, Z., & Arias, I. M. (1969) *J. Clin. Invest. 48*, 2156–2167.

Marquardt, D. W. (1963) *J. Soc. Ind. Appl. Math. 11*, 431–441.
Mishkin, S., & Turcotte, R. (1974a) *Biochem. Biophys. Res. Commun. 57*, 918–926.
Mishkin, S., & Turcotte, R. (1974b) *Biochem. Biophys. Res. Commun. 60*, 376–381.
Mishkin, S., & Roncari, D. A. K. (1976) *Clin. Res. 24*, 682A.
Nichol, L. W., Jackson, W. J. H., & Winzor, D. J. (1967) *Biochemistry 6*, 2449–2456.
Ockner, R. K., & Manning, J. A. (1974) *J. Clin. Invest. 54*, 326–338.
Ockner, R. K., & Manning, J. A. (1976) *J. Clin. Invest. 58*, 632–641.
Ockner, R. K., Manning, J. A., Poppenhausen, R. B., & Ho, W. K. L. (1972) *Science (Washington, D.C.) 177*, 56–58.
O'Doherty, P. J. A., & Kuksis, A. (1975) *FEBS Lett. 60*, 256–258.
Provencher, S. W., & Glöckner, J. (1981) *Biochemistry 20*, 33–37.
Rüstow, B., Kunze, D., Hodi, J., & Egger, E. (1979) *FEBS Lett. 108*, 469–472.
Tanaka, A., Ohnishi, M., & Hiromi, K. (1982) *Biochemistry 21*, 107–113.
Weber, K., & Osborn, M. (1969) *J. Biol. Chem. 244*, 4406–4412.
Wertz, J. E., & Bolton, J. R. (1972) in *Electron Spin Resonance*, pp 197–203, McGraw-Hill, New York.
Wu-Rideout, M. Y. C., Elson, C., & Shrago, E. (1976) *Biochem. Biophys. Res. Commun. 71*, 809–816.

A Nuclear Magnetic Resonance Study of the Topography of Binding Sites of *Escherichia coli* Carbamoyl-phosphate Synthetase†

Frank M. Raushel,‡ Paul M. Anderson, and Joseph J. Villafranca*

ABSTRACT: Two paramagnetic probes, viz., Mn^{2+} and Cr^{3+}-ATP, were used to map distances to various loci on carbamoyl-phosphate synthetase by using NMR measurements. The paramagnetic influence of Mn^{2+} on the ^1H of L-glutamate and L-ornithine was measured at 200 and 360 MHz. On the basis of these data, a correlation time for the paramagnetic interaction was determined (2×10^{-9} s) and used to compute distances. These were in the range 7–9 Å. Distances were also calculated from Mn^{2+} to the ^{13}C-5 atom of glutamate (8.6 Å), to the monovalent cation site (~8 Å), and to the phosphorus atoms of ATP in the $Co(NH_3)_4ATP$ complex. For studies of the monovalent cation site relaxation rates of $^6Li^+$, $^7Li^+$, and $^{15}NH_4^+$ were measured. With $Cr^{3+}ATP$ as a paramagnetic substrate analogue, Cr^{3+} to ^{13}C distances were measured with the substrates HCO_3^- and [5-^{13}C]glutamate. These NMR data provide the first topographical map of the arrangement of substrates, metal ion activators, and allosteric modifiers on the *Escherichia coli* carbamoyl-phosphate synthetase dimer.

Carbamoyl-phosphate synthetase from *Escherichia coli* catalyzes the formation of an important metabolite, carbamoyl phosphate from CO_2, ATP, and a nitrogen source (NH_3 or glutamine depending on the organism). Carbamoyl phosphate is an important precursor for pyrimidine and arginine biosynthesis, and carbamoyl-phosphate synthetase is allosterically regulated in most organisms. In *E. coli*, IMP stimulates activity while UMP inhibits catalysis. Ornithine acts as a potent activator of this enzyme and can overcome inhibition by UMP (Trotta et al., 1973). Thus, regulation of the activity of carbamoyl-phosphate synthetase is crucial for the biosynthesis of nucleic acids and proteins. In higher organisms this enzyme is also important in expulsion of nitrogen via the urea cycle which has arginine as an essential component.

Meister's laboratory (Anderson & Meister, 1966; Trotta et al., 1973) explored the enzymic mechanism in detail and demonstrated that the enzyme requires two molecules of ATP for catalysis and that the overall reaction is given by eq 1.

$$2MgATP + HCO_3^- + \text{L-glutamine} \rightarrow 2MgADP + P_i + \text{L-glutamate} + \text{carbamoyl phosphate} \quad (1)$$

Recent data from our laboratory (Raushel et al., 1978; Raushel & Villafranca, 1979, 1980a,b) and from Wimmer et al. (1979) have established the kinetic mechanism of the enzyme and provided kinetic evidence for the formation of intermediates in the reaction mechanism. These data establish that the intermediates proposed by Anderson & Meister (1965) do indeed form on the enzyme in a kinetically competent manner.

The enzyme has a unique structure in that it is composed of two nonidentical subunits (Matthews & Anderson, 1972; Trotta et al., 1971), the small subunit (M_r ~48 000) possessing the glutamine binding site while the large subunit (M_r ~130 000) contains sites for the other substrates and the allosteric modifiers (Trotta et al., 1971). We have begun a program to map the substrate and allosteric modifier sites by magnetic resonance and fluorescence techniques. Our initial work focused on establishing binding constants for metal ions and substrate analogues as well as labeling specific sulfhydryl

† From the Department of Chemistry, The Pennsylvania State University, University Park, Pennsylvania 16802, and the Department of Biochemistry, School of Medicine, University of Minnesota, Duluth, Duluth, Minnesota 55812. *Received November 19, 1982.* Supported by the U.S. Public Health Service (AM-21785, J.J.V.) (GM-22434, P.M.A.) and the National Science Foundation (PCM-8108094, J.J.V.).

* Address correspondence to this author at The Pennsylvania State University. He is an Established Investigator of the American Heart Association.

‡ Present address: The Department of Chemistry, Texas A&M University, College Station, TX 77840.

0006-2960/83/0422-1872$01.50/0